J Korean Radiol Soc 2003;49:285 - 293

Mediastinal and Hilar Lymphadenopathy: Cross-Referenced Anatomy on Axial and Coronal Images Displayed by Using Multi-detector row CT[1]

Ju-Hyun Lee, M.D., Kyung Soo Lee, M.D., Tae Sung Kim, M.D., Chin A Yi, M.D.
Jae Min Cho, M.D., Min Hee Lee, M.D.

The accurate evaluation of mediastinal and pulmonary hilar lymphadenopathy, especially in patients with lung cancer, is important for determining treatment options and evaluating the response to therapy. To indicate nodal location in detail, mediastinal and hilar lymph nodes have been assigned to one of 14 nodal stations. Mediastinal nodes of greater than 10 mm short-axis diameter are regarded as abnormal, irrespective of their nodal station, while hilar nodes are considered abnormal if their diameter is greater than 10 mm in any axis or they are convex compared to surrounding lung. By providing multiplanar images, multi-detector row CT allows detailed evaluation of thoracic anatomic structures more easily than in the past, when axial images only were available. At cross-referenced imaging, a lymph node depicted at axial imaging in one anatomical location can be visualized simultaneously and automatically at coronal imaging at the exactly corresponding anatomical location. Cross-referenced coincidental axial and coronal images help assess both the size and morphology of mediastinal and hilar lymph nodes.

Index words : Computed tomography (CT), helical
Computed tomography (CT), multi-detector row
Lymphatic system, CT
Mediastinum, CT

The advent of multi-detector row CT (MDCT) offers the advantages of of shorter acquisition time, greater coverage, and superior image resolution at CT imaging (1). Technologic progress has provided the capacity for fast acquisition of volumetric data sets of unprecedented quality and the potential for multi-planar viewing. Currently, multiplanar imaging provides easier access to anatomic details of thoracic structures than in the past, when axial images only were available (2).

The accurate evaluation of mediastinal and pulmonary hilar lymphadenopathy, especially in patients with lung cancer, is important for staging, which is crucial for determining treatment options and evaluating the response to therapy. In addition, evaluation of the presence of extra-capsular invasion of hilar nodal metastasis, which may lead to pneumonectomy or sleeve lobectomy rather than simple lobectomy (5), is important in determining the prognosis and in planning surgery (3, 4).

If only axial images are obtained, mediastinal and hilar lymph node enlargement may not be accurately

[1]Department of Radiology and Center for Imaging Science, Samsung Medical Center, Sungkyunkwan University School of Medicine
Presented as an educational exhibit at the 2002 RSNA scientific assembly
Supported in part by a grant of Korean Research Foundation (Research number 2001-041-F00233)
Received July 14, 2003; Accepted September 15, 2003
Address reprint requests to : Kyung Soo Lee, M.D., Department of Radiology, Samsung Medical Center Sungkyunkwan University School of Medicine, 50, Ilwon-dong, Kangnam-gu, Seoul 135-710, Korea.
Tel. 82-2-3410-2511 Fax. 82-2-3410-2559
E-mail: melon2@samsung.co.kr

identified because the nodal enlargement causing modification of mediastinal or pulmonary hilar morphology may not be entirely evaluated. Multiplanar imaging of the mediastinum or hilum may thus help evaluate accurately the presence of mediastinal and hilar lymph node enlargement. Few details of the coronal anatomy of mediastinal or hilar lymphadenopathy have, however, been published. In this pictorial essay, the authors describe in detail the anatomy of mediastinal and hilar lymphadenopathy, as seen at coronal imaging, co-referencing the information to that depicted by axial images.

Patients and Imaging Technique

During a recent twenty-month period, March 2001 to October 2002, 168 patients in whom central lung malignancy was suspected on the basis of plain chest radiographic findings and physical examination underwent multi-detector row helical CT. A GE Light Speed Qx/i scanner (General Electric Medical Systems, Milwaukee, Wis., U.S.A.) was used, with 2.5-mm detectors, a rotation time of 1.0 second, a pitch of 6, the z-axis of 30 cm that could be covered in 20 seconds. Scans were obtained after the intravenous injection of contrast medium (a total of 80 mL of Iopamidol [Iopamiro 300; Bracco, Milan, Italy]) at a rate of 2.0 mL/sec using an MCT Plus power injector (Medrad, Pittsburgh, Penn., U.S.A.). Imaging data were reconstructed with a thickness of 2.5 mm using a bone algorithm for axial images, and the multiplanar reformation technique was used to obtain coronal views of transaxial CT data sets on a CT workstation (General Electric Medical Systems). Coronal images were reconstructed with 3-mm collimation, and were interactively displayed and edited in real time.

Axial and coronal image data were directly interfaced to a PACS monitor version 8.1 (General Electric Medical Systems Integrated Imaging Solutions, Mt. Prospect, Ill., U.S.A.), allowing cross-referencing of axial and coro-

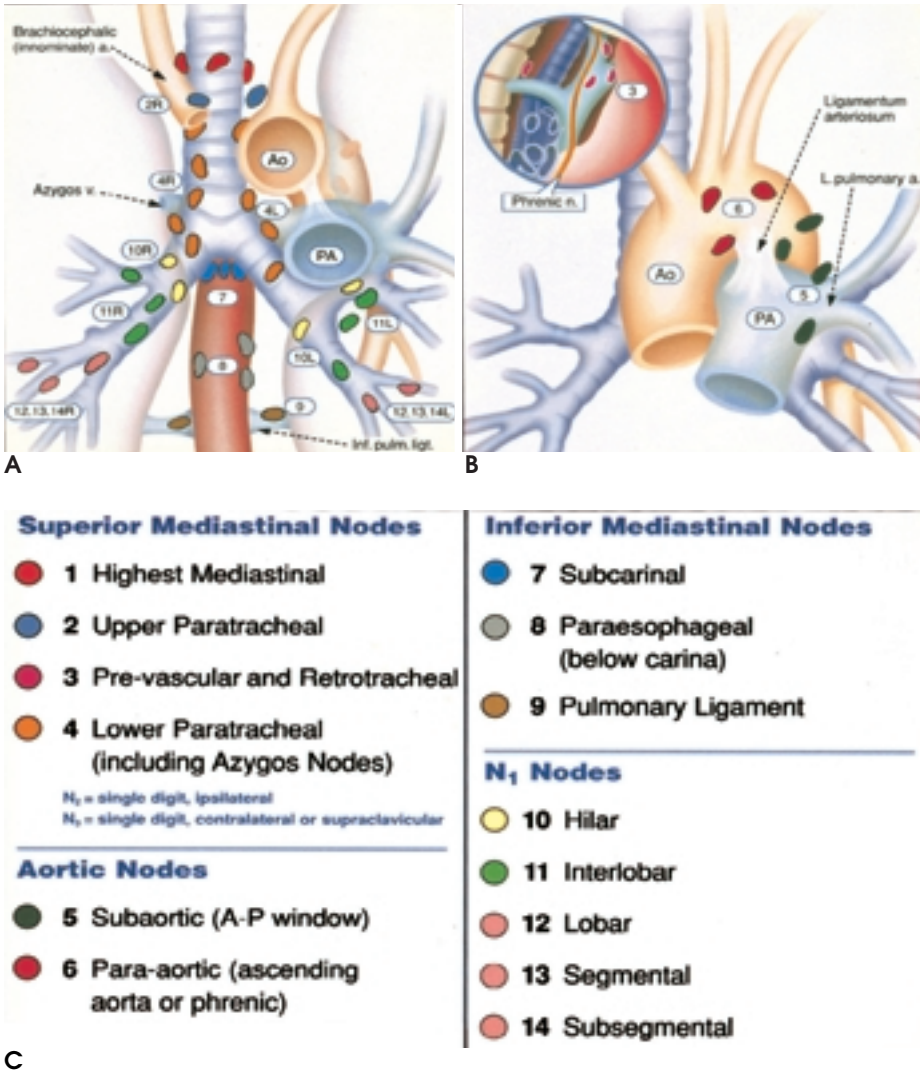

Fig. 1. Nodal station in lung cancer staging. Mediastinum and hilum are viewed from frontal (**A**) and left anterior oblique (**B**) views. Trachea and bronchi, aortic arch (Ao), main pulmonary artery (PA), and esophagus are anatomic landmarks for defining various nodal stations. Nodes occupying nodal stations are assigned various colors, and nodes in corresponding nodal stations on CT scans have also been assigned same colors. Color legends (**C**) for **A** and **B** correlate nodal colors with station numbers and descriptors. Reprinted with permission from reference 8.

nal images. In cross-referencing, if a tool bar of a region of interest (ROI) is moved from one anatomical location to another on axial images in one monitor, exactly corresponding anatomical locations appear simultaneously and automatically on coronal images in the other monitor.

Anatomy of Mediastinal and Hilar Lymph Nodal Enlargement

Hilar (N1) nodes lie within the visceral pleura, and ipsilateral (N2) and contralateral (N3) mediastinal nodes within the mediastinal or parietal pleural reflection (mediastinal pleural envelope). To indicate nodal location in detail, nodes are assigned to one of 14 nodal stations (6 - 8).

Mediastinal Nodes

Mediastinal nodes are assigned to nodal stations 1 - 9. They are subclassified as superior (stations 1-4; station 1 = highest mediastinal nodes, station 2 = upper paratracheal nodes, station 3 = prevascular and retrotracheal nodes, station 4 = lower paratracheal nodes); aortic (stations 5 and 6; station 5 = subaortic or aorticopulmonary window nodes, station 6 = para-aortic [ascending aortic or phrenic] nodes); or inferior (stations 7-9; station 7 = subcarinal nodes, station 8 = paraesophageal nodes, station 9 = pulmonary ligament nodes) (Fig. 1).

SUPERIOR MEDIASTINAL NODES

Station 1 (Highest Mediastinal Nodes)

These lie above a horizontal line at the upper rim of the bracheocephalic (left innominate) vein where it ascends to the left, crossing in front of the trachea at its midline (Fig. 2).

Station 2 (Upper Paratracheal Nodes)

These are found above a horizontal line tangential to the upper margin of the aortic arch and below the inferior boundary of Station 1 nodes (Fig. 3).

Station 3 (Prevascular and Retrotracheal Nodes)

Prevascular nodes are situated anterior to the branches of the great vessel above the superior aspect of the aortic arch, while retrotracheal nodes lie posterior to the

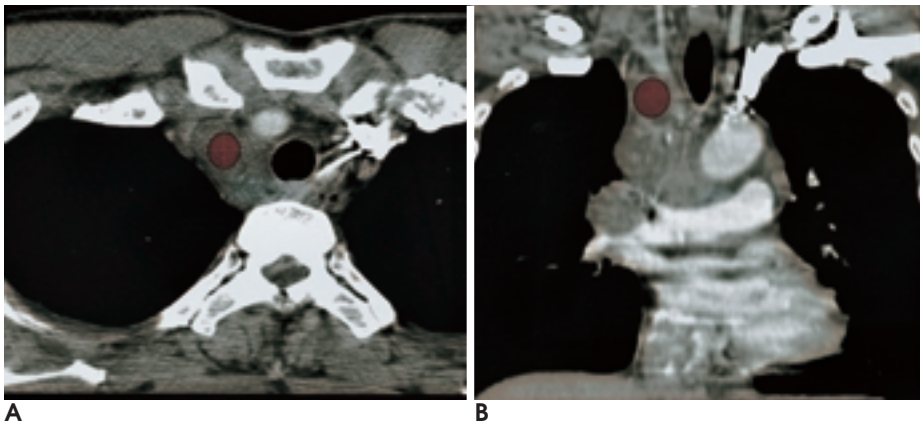

Fig. 2. A 41-year-old man with small cell carcinoma. Axial (**A**) and coronal (**B**) CT scans show highest mediastinal node (colored in red). Nodes are located in right high paratracheal region, lateral to right bracheocephalic artery and medial to right innominate vein. This level is superior to left bracheocephalic vein where it crosses trachea.

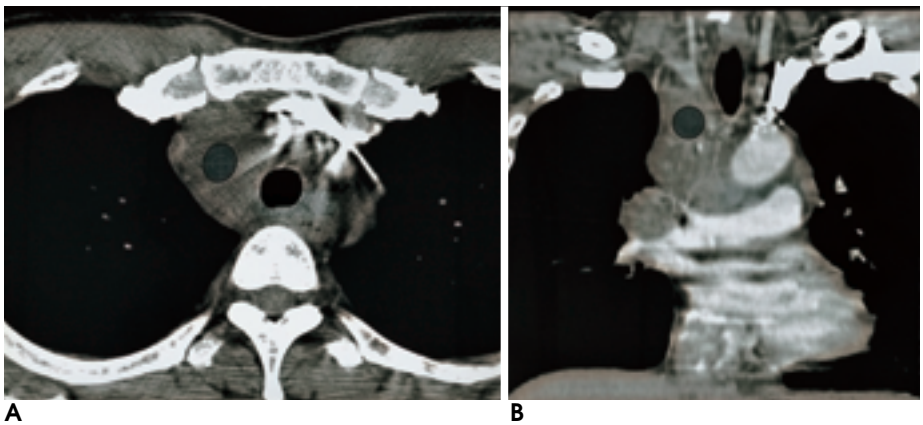

Fig. 3. A 41-year-old man with small cell carcinoma. Axial (**A**) and coronal (**B**) CT scans show right upper paratracheal nodes (colored in blue), which are located inferior to top of left bracheocephalic vein but superior to top of aortic arch.

trachea, below the thoracic inlet and above the inferior aspect of the azygos vein (7) (Fig. 4).

Station 4 (Lower Paratracheal Nodes)

Right lower paratracheal nodes are lie to the right of the midline of the trachea between a horizontal line tangential to the upper margin of the aortic arch and a line extending across the right main bronchus at the upper margin of the upper lobar bronchus, and are contained within the mediastinal pleura (Fig. 5). Left lower paratracheal nodes, on the other hand, are situated to the left of the midline of the trachea between a horizontal line tangential to the upper margin of the aortic arch and a line extending across the left main bronchus at the level

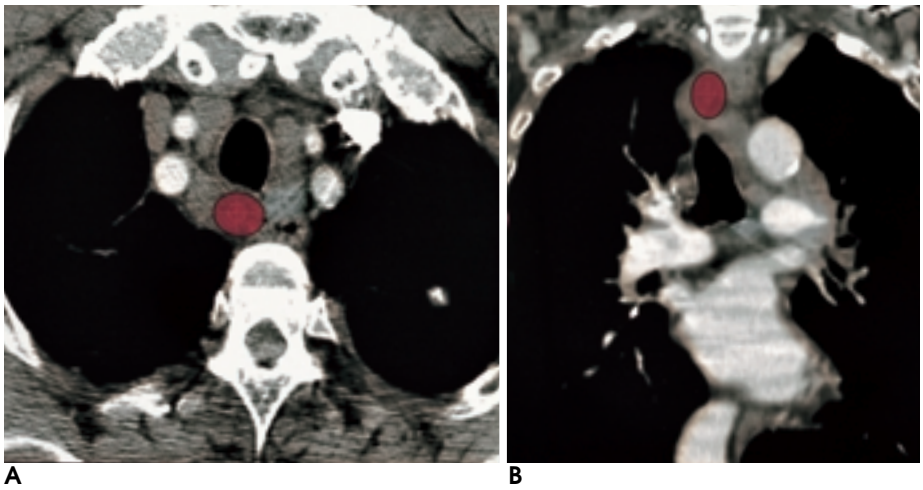

Fig. 4. A 77-year-old man with small cell carcinoma. Axial (**A**) and coronal (**B**) CT scans show retrotracheal nodes (colored in bright pink), lying posterior to trachea at midline.

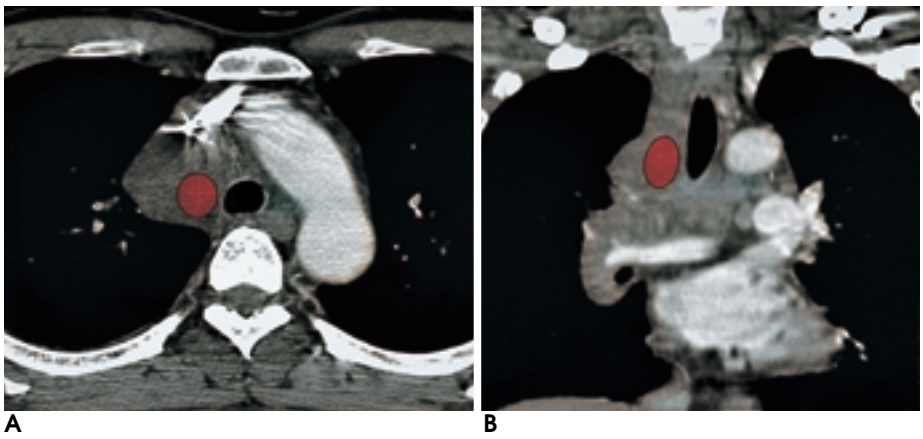

Fig. 5. A 67-year-old man with squamous cell carcinoma. Axial (**A**) and coronal (**B**) CT scans show right lower paratracheal nodes (colored in bright orange), lying right lateral to trachea's midline. This is inferior to superior aspect of aortic arch and superior to superior aspect of right upper lobar bronchus.

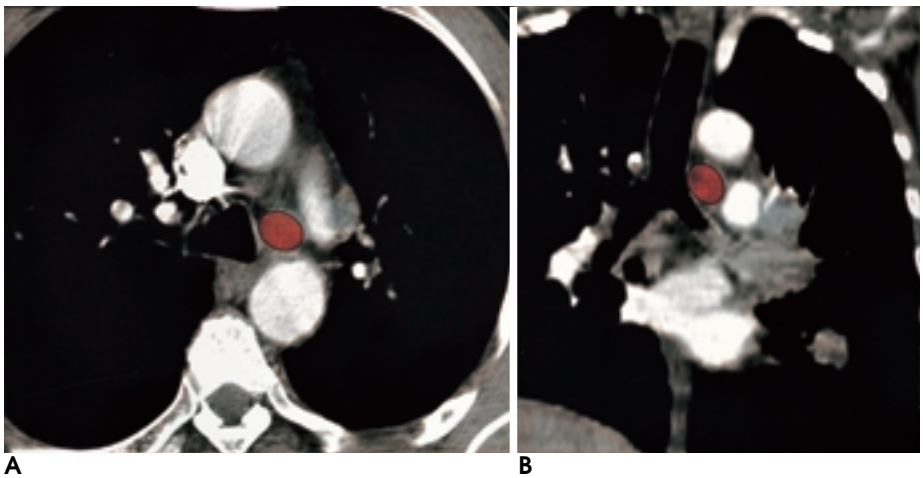

Fig 6. A 58-year-old man with squamous cell carcinoma. Axial (**A**) and coronal (**B**) CT scans show lower paratracheal nodes (colored in bright orange), lying left lateral to trachea's midline. This is inferior to superior aspect of aortic arch and superior to superior aspect of left upper lobar bronchus.

of the upper margin of the left upper lobar bronchus, medial to the ligamentum arteriosum, and are contained within the mediastinal pleural envelope (Fig. 6).

AORTIC NODES

Station 5 (Subaortic Nodes, Aorticopulmonary Window Nodes)

These lie lateral to the ligamentum arteriosum, aorta, or left pulmonary artery, and proximal to the first branch of the left pulmonary artery. They are enclosed by the mediastinal pleural envelope (Fig. 7).

Station 6 (Para-aortic Nodes, Ascending Aortic or Phrenic Nodes)

These are found anterior and lateral to the ascending aorta and the aortic arch or innominate artery, beneath a line tangential to the upper margin of the aortic arch (Fig. 8).

INFERIOR MEDIASTINAL NODES

Station 7 (Subcarinal Nodes)

Subcarinal nodes lie caudal to the carina of the trachea, but are not associated with lower lobe bronchi or arteries within the lung (Fig. 9).

Station 8 (Paraesophageal Nodes)

These are situated adjacent to the wall of the esophagus and to the right or left of the midline, and exclude subcarinal nodes (Fig. 10).

Station 9 (Pulmonary Ligament Nodes)

These lie within the pulmonary ligament, including

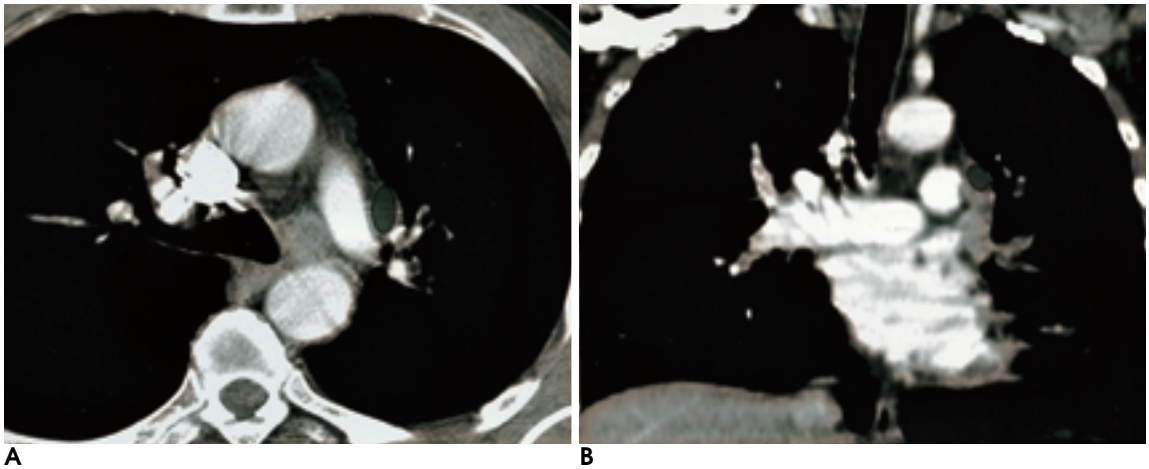

Fig. 7. A 58-year-old man with squamous cell carcinoma. Axial (**A**) and coronal (**B**) CT scan show subaortic nodes (colored in dark green), lying lateral to left pulmonary artery and proximal to first branch of left pulmonary artery.

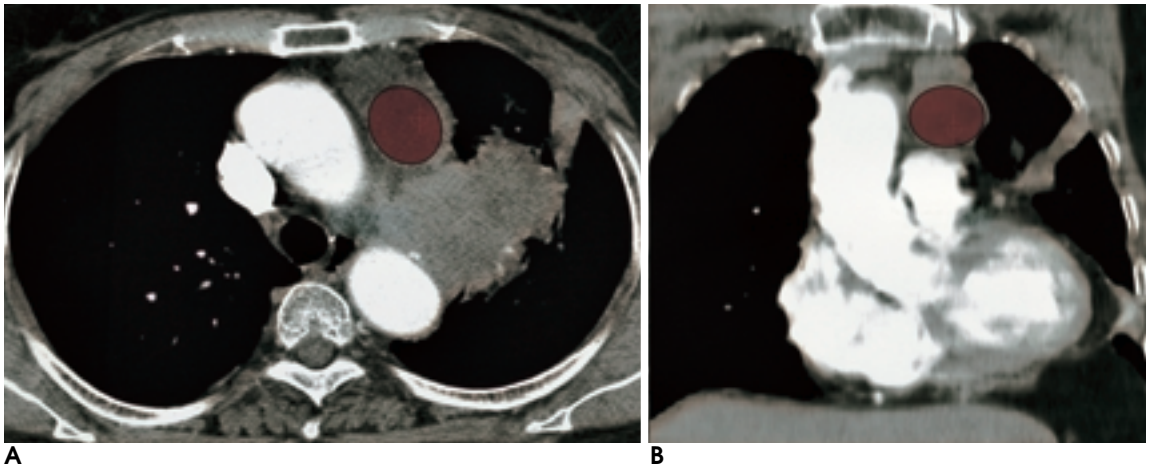

Fig. 8. A 75-year-old woman with small cell lung carcinoma. Axial (**A**) and coronal (**B**) CT scan show para-aortic node (colored in red). Node is lying anterior and lateral to aortic arch, beneath line tangential to upper margin of the aortic arch.

those in the posterior wall and lower part of the inferior pulmonary vein (Figs. 11, 12).

Hilar Nodes

Hilar nodes are assigned to nodal stations 10-14. They are subclassified as station 10 (hilar and proximal lobar nodes), station 11 (interlobar nodes), station 12 (lobar nodes), station 13 (segmental nodes), and station 14 (subsegmental nodes) (Fig. 1).

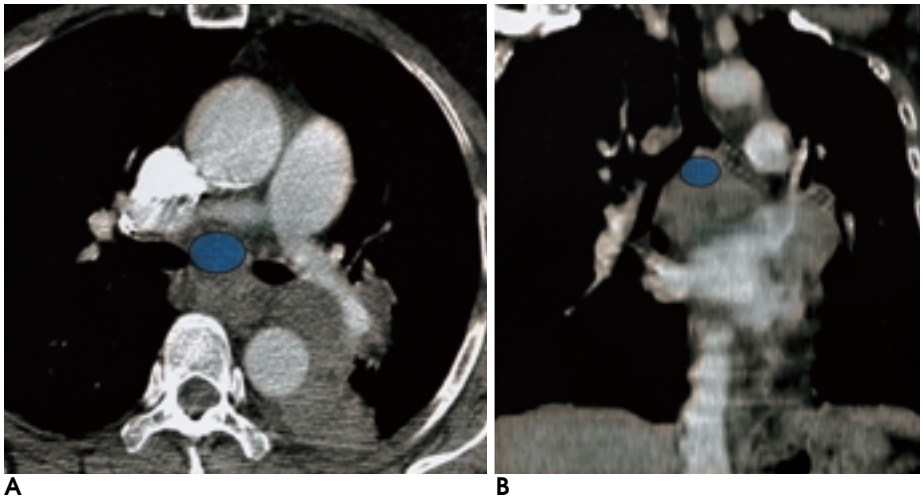

Fig. 9. A 63-year-old woman with small cell carcinoma. Axial (**A**) and coronal (**B**) CT scans show subcarinal nodes (colored in teal blue), located inferior to tracheal carina between main bronchi.

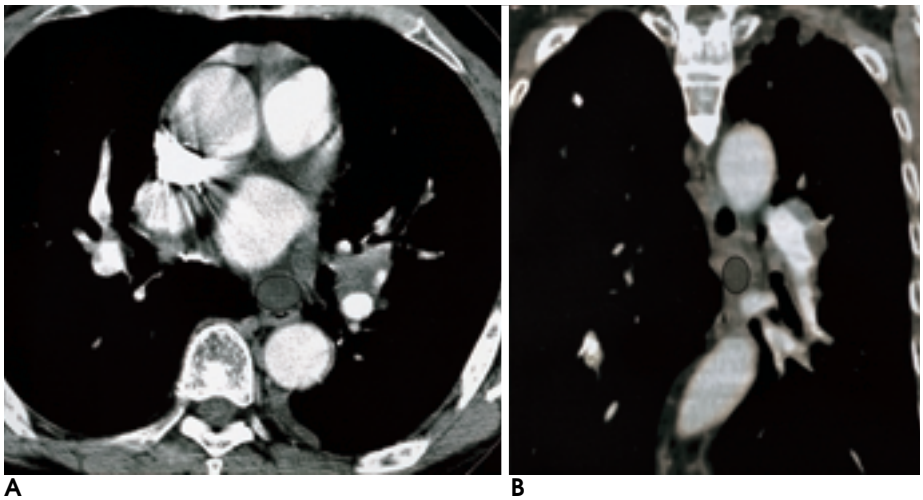

Fig. 10. A 77-year-old man with small cell carcinoma. Axial (**A**) and coronal (**B**) CT scans show paraesophageal node (colored in gray), lying anterolateral to azygos vein and anterior to esophagus.

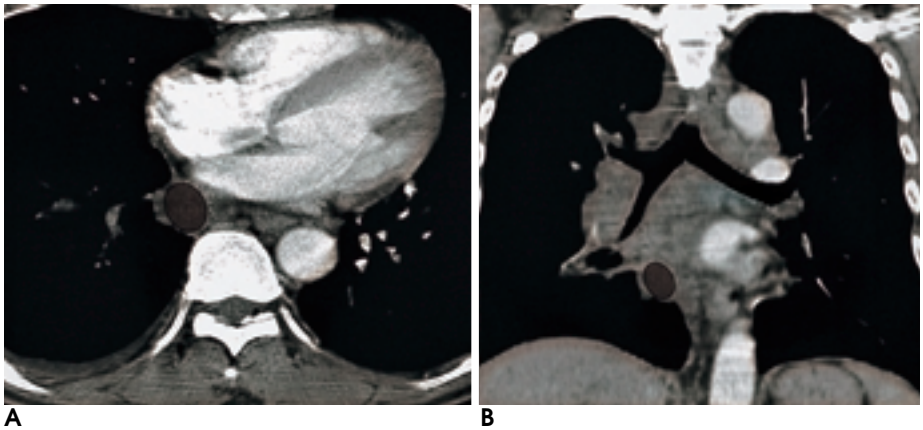

Fig. 11. A 60-year-old man with small cell carcinoma. Axial (**A**) and coronal (**B**) CT scans show right inferior pulmonary ligament nodes (colored in tan).

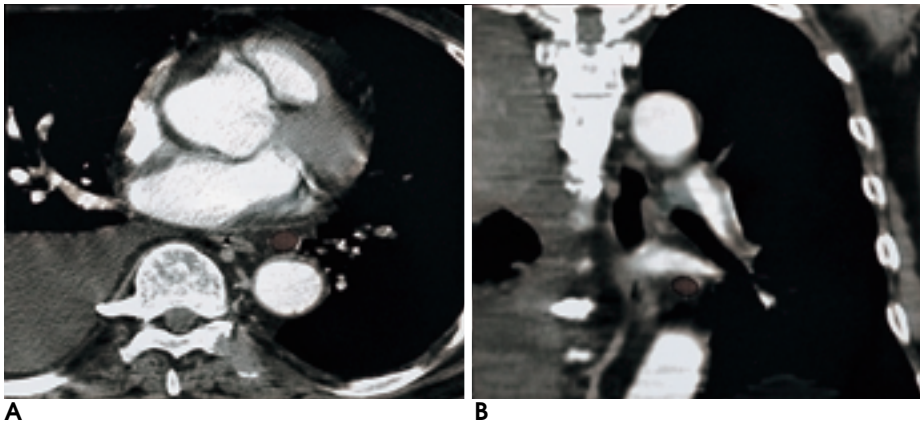

Fig. 12. A 68-year-old man with adenocarcinoma of right upper lobe. Axial (**A**) and coronal (**B**) CT scans show left inferior pulmonary ligament nodes (colored in tan).

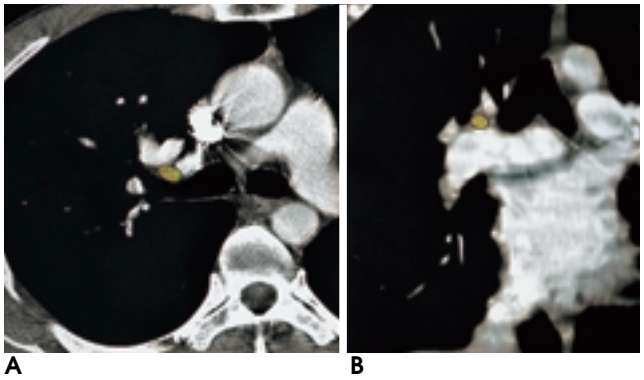

Fig. 13. A 45-year-old man with metastatic lymphadenopathy. Axial (**A**) and coronal (**B**) CT scans show right hilar node (colored in yellow), lying anterior to right upper lobar bronchus, posterior to anterior segmental branch of truncus anterior. Nodes are located superior to the right upper pulmonary artery.

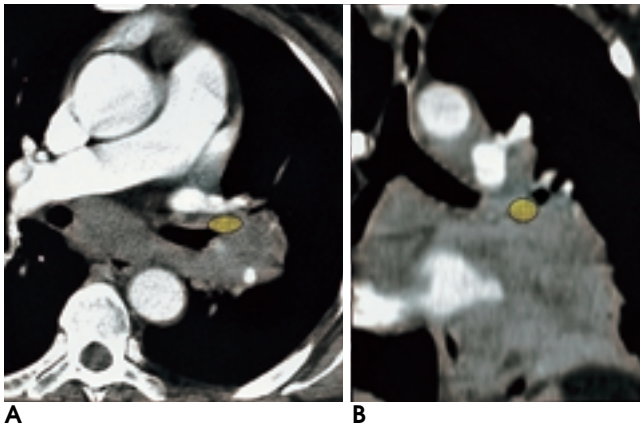

Fig. 14. A 53-year-old woman with small cell carcinoma. Axial (**A**) and coronal (**B**) CT scan show left hilar node (colored in yellow). Node is lying anterior to distal left main bronchus and inferior to proximal left pulmonary artery.

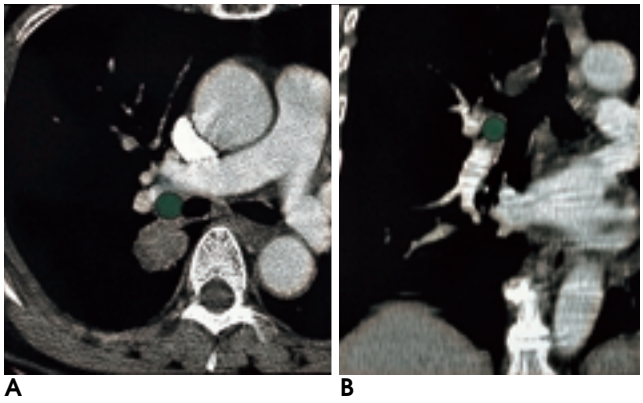

Fig. 15. A 61-year-old woman with adenocarcinoma of right upper lobe. Axial (**A**) and coronal (**B**) CT scans show right interlobar node (colored in green), located medial to right central vein, lateral to bronchus intermedius, and slightly posterior and superior to right interlobar artery. Nodes are located superior to right interlobar artery and inferior to right upper lobar bronchus.

Station 10 (Hilar or Proximal Lobar Nodes)

Right hilar nodes are located caudal to the superior aspect of the right upper lobe bronchus and lie adjacent to the right main bronchus and the proximal bronchus intermedius. Similarly, left hilar nodes are caudal to the superior aspect of the left upper lobe bronchus and adjacent to the left main bronchus (Figs. 13, 14).

Station 11 (Interlobar Nodes)

These are found between lobar bronchi and are adjacent to the proximal lobar bronchi (Figs. 15, 16). Right interlobar nodes are those which lie alongside the bronchus intermedius, and are posterior or posterior and superior to the right interlobar artery, slightly inferior to the right hilar nodes, and in the right major fissure between the upper and lower lobes (9) (Fig. 15). They are also known as "sump nodes of Borrie" (4). In this area of right interlobar nodes or sump nodes of Borrie, there may be normal prominent soft-tissue collections without significant nodal enlargement, which simulate

lymphadenopathy or pulmonary embolism (10). Left interlobar nodes are located between the lingular segmental bronchus and interlobar artery, or between the left lower lobe and interlobar artery (9) (Fig. 16).

Station 12 (Lobar Nodes)

These are found

adjacent to the distal portions of lobar bronchi (Fig. 17).

Station 13 (Segmental Nodes)

These are

adjacent to the segmental bronchi (Fig. 18).

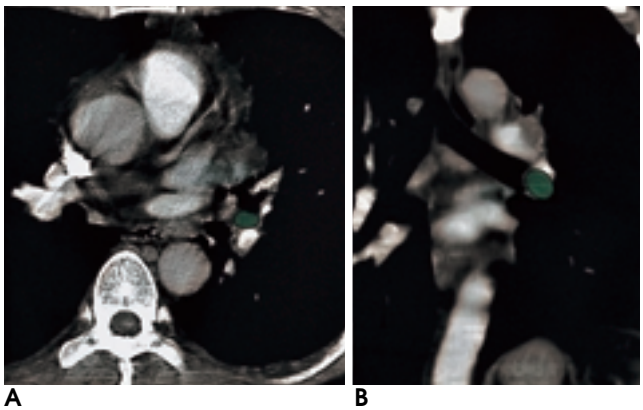

A B

Fig. 16. A 51-year-old man with small cell carcinoma. Axial (**A**) and coronal (**B**) CT scans show left interlobar node (colored in green), lying between lingular segmental bronchus and left interlobar artery on axial scan and between left lower lobar bronchus and lingular segment of left upper lobe on coronal scan. Nodes are located inferior to left interlobar artery.

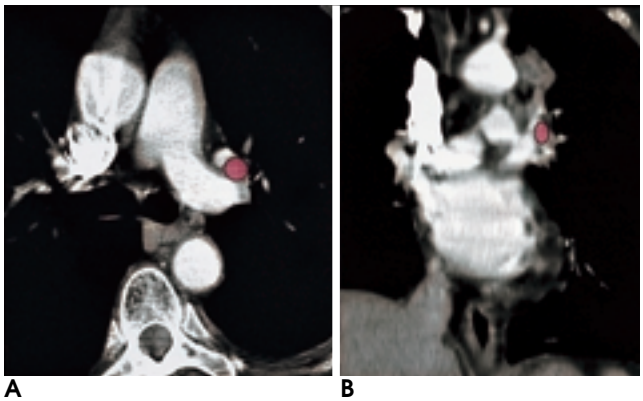

A B

Fig. 17. A 65-year-old woman with adenocarcinoma of left upper lobe. Axial (**A**) and coronal (**B**) CT scans show left upper lobar nodes (colored in light pink), lying between main pulmonary artery and left superior pulmonary vein. Nodes are located between main pulmonary artery medially and apicoposterior segmental bronchi laterally. On coronal images, nodes are located between apicoposterior segmental vein of left upper lobe superiorly and anterior segmental vein inferiorly.

Station 14 Subsegmental Nodes

These, too, are adjacent to the subsegmental bronchi (Fig. 19).

CT Diagnostic Criteria of Mediastinal and Hilar Lymphadenopathy

At CT, the most reliable and practical measurement of lymph node size is the short-axis diameter, which correlates better than the long-axis diameter with node volume and is less influenced by the spatial orientation of the node. Although some investigators have suggested the use of various nodal size criteria specific for each mediastinal nodal station, for practical reasons a short-axis diameter greater than 10 mm is generally regarded as abnormal, irrespective of the nodal station (11-13). The size and morphologic diagnostic criteria of hilar

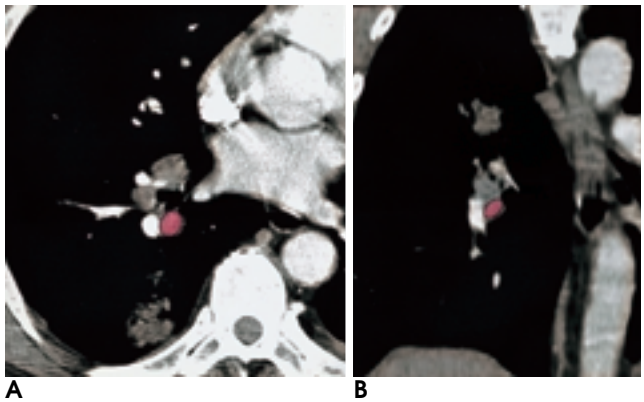

A B

Fig. 18. A 59-year-old man with small cell carcinoma. Axial (**A**) and coronal (**B**) CT scan show right lower lobar nodes (colored in light pink), lying between basal segmental arteries and veins, outer to basal segmental bronchi. On coronal images, nodes are located between segmental arteries and veins, outer to basal segmental bronchi.

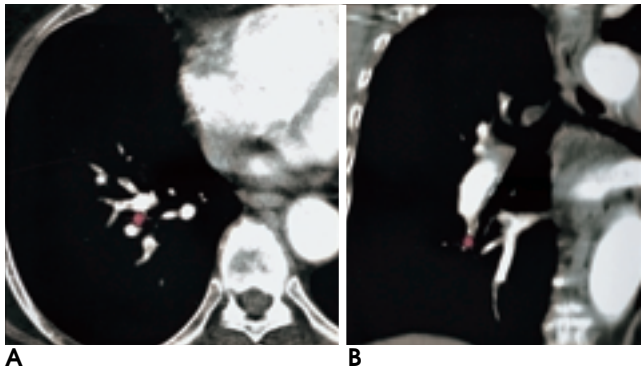

A B

Fig. 19. A 75-year-old woman with small cell carcinoma. Axial (**A**) and coronal (**B**) CT scan show right subsegmental node (colored in light pink). Node is lying adjacent to subsegmental bronchi.

lymph node enlargement have been suggested (2,5): Glazer et al. (14) proposed that a diameter greater than 10 mm should be considered abnormal, the same nodal criterion used for the diagnosis of mediastinal nodal metastasis; more recently, Shimoyama et al. (5) suggested that in lung cancer patients, hilar nodes which are convex to surrounding lung are positive for metastasis. However, neither size nor the morphologic diagnostic criterion of hilar node enlargement is completely satisfactory in the diagnosis of hilar lymphadenopathy.

References

1. Lawler LP, Fishman EK. Multi-detector row CT of thoracic disease with emphasis on 3D volume rendering and CT angiography. *Radiographics* 2001;21:1257-1273
2. Remy-Jardin M, Remy J. Spiral CT angiography of the pulmonary circulation. *Radiology* 1999;212:615-636
3. Kaiser LR, Shrager JB. Video-assisted thoracic surgery: the current state of the art. *AJR Am J Roentgenol* 1995;165:1111-1117
4. Murray GF, Mendes OC, Wilcox BR. Bronchial carcinoma and the lymphatic sump: the importance of bronchoscopic findings. *Ann Thoracic Surg* 1982;34:634-639
5. Shimoyama K, Murata K, Takahashi M, Morita R. Pulmonary hilar lymph node metastases from lung cancer: evaluation based on morphology at thin-section, incremental, dynamic CT. *Radiology* 1997;203:187-195
6. Cymbalista M, Waysberg A, Zacharias C, et al. CT demonstration of the 1996 AJCC-UICC regional lymph node classification for lung cancer staging. *Radiographics* 1999;19:899-900
7. Ko JP, Drucker EA, Shepard JA, et al. CT depiction of regional nodal stations for lung cancer staging. *AJR Am J Roentgenol* 2000;174:775-782
8. Mountain CF, Dresler CM. Regional lymph node classification for lung cancer staging. *Chest* 1997;111:1718-1723
9. Sone S, Higashihara T, Morimoto S, et al. CT anatomy of hilar lymphadenopathy. *AJR Am J Roentgenol* 1983;140:887-892
10. Ashida C, Zerhouni EA, Fishman EK. CT demonstration of prominent right hilar soft tissue collection. *J Comput Assist Tomogr* 1987; 11:57-59
11. Quint LE, Glazer GM, Orringer MB, Francis IR, Bookstein FL. Mediastinal lymph node detection and sizing at CT and autopsy. *AJR Am J Roentgenol* 1986; 147:469-472
12. Buy JN, Ghossain MA, Poirson F, et al. Computed tomography of mediastinal lymph nodes in nonsmall cell lung cancer. A new approach based on the lymphatic pathway of tumor spread. *J Comput Assist Tomogr* 1988;12:545-552
13. Ikezoe J, Kadowaki K, Morimoto S, et al. Mediastinal lymph node metastases from non-small cell bronchogenic carcinoma: reevaluation with CT. *J Comput Assist Tomogr* 1990;14:340-344
14. Glazer GM, Gross BH, Aisen AM, Quint LE, Francis IR, Orringer MB. Imaging of the pulmonary hilum: a prospective comparative study in patients with lung cancer. *AJR Am J Roentgenol* 1985;145: 245-248

대한방사선의학회지 2003;49:285 - 293

종격동과 폐문 림프절병증: Multi-detector row CT를 이용한 축면스캔과 관상면스캔의 교차 대응 해부[1]

[1]성균관대학교 의과대학 방사선과학교실

이주현 · 이경수 · 김태성 · 이진아 · 조재민 · 이민희

종격동과 폐문 림프절병증의 정확한 평가는 특히 폐암환자에서 치료 방법 선택과 치료에 대한 반응을 평가하는데 중요하다. 이러한 림프절의 상세한 위치는 14개로 분류되며 종격동 림프절은 단경 10 mm 이상일때 비정상으로 간주한다. 폐문 림프절의 경우는 방향과 상관없이 10 mm 이상이거나 주위 폐에 대해 볼록함을 보일 때 비정상으로 간주한다. 축면스캔만 유효했던 종전과 비교할 때 multi-detector row CT를 이용한 다평면영상으로 흉부해부구조의 세부적 평가가 더 용이해졌다. 교차 대응영상으로 축면스캔에서의 림프절 위치가 동시에 자동적으로 관상면스캔에 정확히 표시되며 이를 이용하면 종격동과 폐문 림프절의 크기와 모양의 평가에 도움이 된다.